JOURNAL OF OCULAR PHARMACOLOGY AND THERAPEUTICS
Volume 34, Number 3, 2018

DOI: 10.1089/jop.2017.0059

Targeting HDAC3 Activity with RGFP966 Protects Against Retinal Ganglion Cell Nuclear Atrophy and Apoptosis After Optic Nerve Injury

Heather M. Schmitt,[1,2] Cassandra L. Schlamp,[1] and Robert W. Nickells[1]

Abstract

Purpose: HDAC3 regulates nuclear atrophy as an early response to axonal injury in retinal ganglion cells (RGCs) following optic nerve crush (ONC). Since conditional knockout of *Hdac3* prevents nuclear atrophy post ONC, HDAC3 selective inhibition with RGFP966 through localized and systemic dosing of RGFP966 is necessary for application to acute and chronic models of optic nerve injury.
Methods: C57BL/6 mice were injected intravitreally with 1–10 μM RGFP966 immediately following ONC, and retinas were analyzed at 5, 7, and 14 days for metrics of nuclear atrophy and cell loss. Mice were similarly assessed after intraperitoneal (IP) injections with RGFP966 doses of 2–10 mg/kg, and eyes were harvested at 5, 14, and 28 days after ONC. H&E and BrdU staining were used to analyze toxicity to off-target tissues after 14 days of daily treatment with RGFP966.
Results: A single intravitreal injection of RGFP966 prevented histone deacetylation, heterochromatin formation, apoptosis, and DNA damage at 5 and 7 days post ONC. After IP injection, RGFP966 bioavailability in the retina reached peak concentration within 1 h after injection and then rapidly declined. A single IP injection of 2–10 mg/kg RGFP966, significantly prevented histone deacetylation. Repeated IP injections of 2 mg/kg RGFP966 over the course of 2 and 4 weeks post ONC prevented RGC loss. There were no significant toxic or antiproliferative effects to off-target tissues in mice treated daily for 14 days with RGFP966.
Conclusion: Inhibition of HDAC3 activity with systemic dosing of RGFP966 prevents apoptosis-related histone deacetylation and attenuates RGC loss after acute optic nerve injury.

Keywords: retinal ganglion cell, histone deacetylase 3 (HDAC3), neurodegeneration, epigenetics, neuroprotection, apoptosis

Introduction

GLAUCOMA, A PREVALENT optic neuropathy that leads to blindness, arises as a result of ocular hypertension-induced axonal damage at the optic nerve head, inducing retinal ganglion cell (RGC) death. A commonly used model of acute axonal damage to RGCs is rodent optic nerve crush (ONC).[1] In this model, the stages of apoptosis can be readily assessed due to the synchronous manner in which RGC death occurs from the crush insult to the optic nerve. The early stages of nuclear atrophy, including histone deacetylation and heterochromatin formation, have been shown to precede the BAX-dependent step in RGC apoptosis.[2,3]

Histone deacetylases (HDACs) affect gene expression by removing acetyl groups from lysine residues on histones, which regulates chromatin remodeling during cellular development, differentiation, and death.[4,5] Class I HDACs 1, 2, and 3 are ubiquitous in the retina and are upregulated following axonal injury.[3,6] HDAC3 was shown to translocate to the nucleus from the cytoplasm of RGCs early after axonal injury,[3,7] coinciding with the period of maximal histone deacetylation after injury. The importance of HDAC3 in this process was confirmed by conditional knockout of *Hdac3* in RGCs, which prevented global histone deacetylation and heterochromatin formation, and attenuated apoptosis in RGCs following axonal injury.[8]

The finding that HDAC3 activity is a critical regulator in RGC atrophy is congruent with the reports that HDAC3 activity has been found to be neurotoxic, and HDAC3 has become a prime target for therapeutics to treat neurodegenerative diseases such as Friedrich's ataxia, Huntington's disease, and memory loss.[9–12] While broad-spectrum HDAC

[1]Department of Ophthalmology and Visual Sciences, University of Wisconsin–Madison, Madison, Wisconsin.
[2]Cellular and Molecular Pathology, University of Wisconsin–Madison, Madison, Wisconsin.

inhibition in the retina has been shown to protect against RGC death in models of acute and chronic optic nerve damage,[3,6,7,13,14] selective inhibition of HDACs may provide clearer insight into the roles of individual HDACs as well as provide a more targeted therapeutic approach against detrimental HDACs.

In this study, we test the HDAC inhibitor RGFP966, which can pass through the blood–brain barrier,[12] in the mouse ONC model. This inhibitor has a high affinity for HDAC3, and moderate affinities for HDACs 1 and 2,[12] and has been used in preclinical testing in other models of neuronal degeneration.[15] Localized intravitreal injections and systemic injections of specific doses of the drug prevents histone deacetylation, heterochromatin formation, and is protective to RGCs following axonal damage. The results indicate that therapeutic levels of RGFP966 are present in the retina within 1 h of systemic injection, and animals treated daily with 10 mg/kg doses of RGFP966 showed no pathological side effects from the treatment. The data from these experiments provide the groundwork for preclinical application of RGFP966 to prevent RGC death in chronic models of glaucoma.

Methods

Experimental animals, RGFP966 injection, and ONC

All mice were handled in accordance with the Association for Research in Vision and Ophthalmology statement for the use of animals for research, and experimental protocols were approved by the Institutional Animal Care and Use Committee (IACUC) of the University of Wisconsin–Madison. A random mixture of male and female C57BL/6 mice, between the ages of 4 and 6 months, was used for experiments. To initiate the degeneration of RGCs, ONC was performed unilaterally on the left eyes of mice using self-closing forceps as described previously.[16]

A slow-on slow-off tight-binding HDAC3 inhibitor, RGFP966, was provided by Repligen Corporation (Waltham, MA) and BioMarin (San Rafael, CA). RGFP966 crosses the blood–brain barrier and has an IC_{50} value of 0.064 μM for HDAC3 (Table 1).[12] RGFP966 was diluted to 1.0, 2.0, 7.0, and 10.0 μM (equivalent to 1.0, 2.0, 7.0, and 10.0 pmol/μL) by mixing in vehicle solvent [5% dimethyl sulfoxide (DMSO), 30% 2-hydroxypropyl-beta-cyclodextrin (HPβCD), and 0.1 M acetate (pH 5.4)]. Using a NanoFil syringe with a 35-gauge beveled needle, mice were given an intravitreal injection of 1.0 μL of the HDAC3-specific inhibitor RGFP966 or vehicle alone into the OS eye immediately following ONC.

The calculated final concentrations of RGFP966 in the vitreous after direct injection were 0.19, 0.37, 1.27, and 1.82 μM, based on an estimated total vitreous volume of 5.4 μL. The OD eyes served as uninjured and untreated controls. Peak histone deacetylation occurs 5 days after ONC.[3] Therefore, retinas were harvested 5 days after ONC to measure histone H4 deacetylation, and heterochromatin formation. For cell death-related metrics, retinas were collected 7 days after ONC to assess DNA damage by terminal transferase dUTP nick end labeling (TUNEL), which is when others have shown maximum TUNEL labeling.[16] Retinas were also collected 14 days after ONC for total cell counts.

A single systemic injection of RGFP966 was administered intraperitoneally (IP) immediately after ONC. A stock solution of 1 mg/mL RGFP966 in 5% DMSO in HPβCD vehicle was made, and mice were weighed before administering the drug solution appropriately with no more than a volume of 10 μL/g of mouse, as per IACUC guidelines. For example, a mouse weighing 23.6 g would be IP injected with 236 μL of stock solution (containing 0.236 mg RGFP966) for a single 10 mg/kg dose. RGFP966 was dosed to 2, 6, and 10 mg/kg of mouse, and retinas were harvested at 5 days following ONC to measure histone deacetylation as a dose–response. To assess a prolonged treatment paradigm, IP injections of vehicle (100 μL), 2 or 10 mg/kg were administered daily, every 3 days, and every 7 days following ONC. Retinas were then harvested 2 and 4 weeks after ONC to assess histone H4 deacetylation, BRN3A labeling, and cell loss in the ganglion cell layer (GCL).

Immunofluorescence

Enucleated eyes were fixed in 4% paraformaldehyde in phosphate-buffered saline (PBS) (150 mM NaCl, 100 mM NaH_2PO_4, pH 7.4) for 1 h before rinsing with PBS and whole mounting. Retinas were isolated from these eyes, given 4 relaxing cuts, and then mounted on Superfrost Plus microscope slides (Fisher Scientific, Hampton, NH) with the GCL facing up, and rinsed again in PBS. The whole mounts were then blocked in 5% bovine serum albumin and 2% Triton X-100 in PBS for 3 h at room temperature in humidified chambers before rinsing with PBS. Primary antibodies included a polyclonal rabbit antibody to human AcH4 (Cat No. 06-866, RRID: AB_310270), a monoclonal mouse antibody to human brain-specific homeobox/POU domain protein 3A (BRN3A) (Cat No. MAB1585, RRID: AB_94166) (both from EMD Millipore, Inc., Billerca, MA), and monoclonal mouse antibody to human Beta III Tubulin (TUJ-1) (Cat No. ab14545) (Abcam, Cambridge, MA). Whole mounts were incubated in 1:50 (for BRN3A) or 1:100 primary antibody in 5% BSA 0.1% Triton X-100 in PBS for 24 hours at 4°C and washed in PBS afterwards. Secondary antibodies used included goat anti-rabbit TEXAS RED (1:1,000), goat anti-mouse FITC, and goat anti-mouse Alexa-488 (Jackson ImmunoResearch Laboratories, West Grove, PA) in PBS. Whole mounts were incubated in secondary antibody at room temperature in the dark for 2 hours and washed in PBS. All whole mounts were counterstained for 10 min with 300 ng/mL 4′, 6-diamidino-2-phenylindole (DAPI) before washing with PBS. Lastly, whole

Table 1. RGFP966 is an HDAC3 Selective Inhibitor

Inhibitor	*Molar mass*	*Blood–brain barrier permeable?*	*HDAC1*	*HDAC2*	*HDAC3*
RGFP966	362.4 g/mol	Yes	IC50 2.069 μM = 1.97 nmol/g retinal tissue	IC50 3.961 μM = 3.77 nmol/g retinal tissue	IC50 0.064 μM = 0.061 nmol/g retinal tissue

mounts were mounted using Immumount mounting medium (Fisher Scientific) and coverslipped. Fluorescent images were obtained using a Zeiss Axioplan 2 Imaging microscope with AxioVision 4.6.3.0 software (Carl Zeiss MicroImaging, Inc., Thornwood, NY). Cell counts were done by collecting digital images at 400× magnification of each retinal lobe with cell nuclei stained with DAPI, and cell numbers were determined in 24 separate 100 μm^2 fields for each retina. Only cells with rounded or oval nuclei, containing prominent nucleoli, were counted because these represent either RGCs or displaced amacrine neurons. We estimate that this method samples between 5% and 10% of the neurons in the GCL of the average normal mouse retina. The change in cell number for each experimental eye was calculated as a percentage of cell numbers in corresponding control eyes.

TUNEL, BrdU, and H&E labeling

To assess DNA damage in the GCL at 7 days post ONC, eye cups were harvested, fixed in 4% paraformaldehyde in PBS for 1 h, rinsed in PBS, and retinas were whole mounted. Retinas were then labeled with TUNEL using the DeadEnd TUNEL Kit from Promega Co. (Madison, WI). All whole mounts were counterstained for 10 min with 300 ng/mL DAPI before washing with PBS. Lastly, whole mounts were mounted using Immumount mounting medium (Fisher Scientific) and coverslipped. Fluorescent images were obtained using a Zeiss Axioplan 2 Imaging microscope with AxioVision 4.6.3.0 software (Carl Zeiss MicroImaging, Inc.). Cell counts in retinal whole mounts were conducted as described above and all cells showing at least some level of TUNEL staining associated with a DAPI-positive nucleus were counted as being positive.

To assess proliferation of cell populations in tissues of mice treated systemically for 14 days with 10 mg/kg RGFP966 or vehicle, mice were injected with 2 mg BrdU (Fisher Scientific) 24 h before euthanasia. After euthanasia, harvested small intestinal tissue sections (inferior to the duodenum) were rinsed in ice cold PBS and incubated in 10% neutral buffered formalin for 24 h at room temperature. Intestinal tissues were then placed in cassettes and incubated in 70% ethanol for 48 h before embedding in paraffin and sectioning. Slides were then deparaffinized in ethanol washes, rinsed in PBS, blocked in 3% H_2O_2 in PBS for 2 h, rinsed again in PBS, permeabilized in 0.05% trypsin in H_2O at 37°C for 10 min, rinsed in PBS, and labeled for BrdU using the BrdU *In Situ* Detection Kit from BD Pharmingen (BD Biosciences, San Jose, CA). Slides were then incubated in Hematoxylin for 60 s and rinsed in H_2O thoroughly before coverslipping and imaging using the Zeiss Imager A2 (Carl Zeiss MicroImaging, Inc.) and a digital camera attachment.

Cell counts of BrdU-labeled cells in treated and untreated mouse intestinal crypts were collected by first taking 10 digital images (fields) at 200× magnification. Then, using ImageJ software to do particle threshold and watershed adjustment to separate neighboring nuclei, the particle analysis plug-in was utilized to export total BrdU-positive cell numbers within each 200 μm^2 region. Cell numbers from each of 10 fields per treatment group were analyzed to produce a mean value of BrdU-positive cells per field for each treatment group.

Systemic tissues were evaluated by H&E staining after daily IP injection with vehicle or 10 mg/kg RGFP966 for 14 days in mice ($n=5$ per treatment group). After euthanasia, tissues from the heart, lung, liver, kidney, small intestine, skin, and brain were surgically removed, rinsed in PBS, and fixed in 10% neutral buffered formalin for 24 h at room temperature. After fixation, tissues were placed in cassettes (Fisher Scientific) and incubated in 70% EtOH for 48 h before paraffin embedding and sectioning. Slides were then deparaffinized in xylene, rehydrated in ethanol washes, stained in Modified Harris Hematoxylin (Fisher Scientific), washed in water, differentiated (excess dye in tissue was selectively removed) in 2%–3% acid alcohol, washed in water, blued in saturated lithium carbonate solution, washed in water, rinsed in 70% EtOH, counterstained in Eosin solution, dehydrated in alcohol changes and xylene, and mounted in xylene-based medium. Slides were then analyzed by a veterinary pathologist for any indication of abnormalities such as cellular vacuolization, inflammation, apoptosis, or necrosis.

Transmission electron microscopy

C57BL/6 mouse OS eyes were intravitreally injected with 1 μL of HPβCD vehicle, 2, or 10 μM RGFP966 immediately following ONC ($n=3$ per treatment group). OS (ONC) and OD (contralateral) eyes then harvested 5 days following ONC, and enucleated eyes were fixed in 4% paraformaldehyde in 0.1 M phosphate buffer (PB) for 5 min, after which the anterior chambers and lenses were dissected away from each eyecup. A small region of the superior eyecup was then removed and placed in 2.5% glutaraldehyde, 2% paraformaldehyde in 0.1 M PB pH 7.4 (PB) overnight at 4°C. The division of the superior region of the eyecup was done to allow for complete submersion of the tissue in the Epon epoxy block for sectioning and previous studies have shown that changes in this region of the retina consistently reflect the overall damage produced by ONC surgery.[16] Tissues were postfixed in 1% osmium tetroxide in PB, dehydrated in ethanol, and embedded in Epon epoxy. Sections (60–90 nm) were cut, stained with 50% ethanoic uranyl acetate and Reynold's lead citrate, and viewed using a Phillips CM120 transmission electron microscope (FEI Company, Hillsborn, OR).

Heterochromatin scoring analysis

Retinas processed for transmission electron microscopy (TEM) were also sectioned for bright-field microscopy. Thick (1 μm) sections were cut from epoxy-embedded samples and stained with Richardson's stain (Methylene Blue and Azure Blue). Sections were imaged using Olympus BX40 light microscope (Olympus Corporation, Center Valley, PA) and a digital camera attachment. Nuclear morphology of cells in the GCL was scored by 2 masked observers. A score of 1 indicated healthy cells with euchromatic nuclei and well-formed nucleoli; a score of 2 indicated partially heterochromatic cells; and a score of 3 indicated cells with completely condensed and pyknotic chromatin. Scoring counts were done on 400× magnified digital images of sections and were collected from ~10 to 20 images per section. Counts from 30 to 60 images per treatment group were analyzed and the distribution of cells with each score was calculated as a percent of the total cells counted in that treatment group.

Mass spectrometry

Mice were injected IP with 2 mg/kg at 0, 0.25, 0.5, 1, 2, 6, and 24 h or 10 mg/kg RGFP966 at 0, 1, 2, 6, and 24 h before

euthanasia ($n=3$ per time point). Retinas were harvested, submerged in ice-cold 1:100 serine protease inhibitor phenylmethanesulfonyl fluoride (PMSF) in PBS, weighed, and homogenized by sonication. Retinal homogenates with volumes of 120 μL were diluted 6-fold with acetonitrile to 720 μL, vortexed, and placed on ice for 1 h. Samples were centrifuged at 16,000 *g* for 5 min at room temperature and the supernatants removed. Calibration curve samples were created by taking 3 additional retina homogenates from untreated animals and spiking with 1, 25, and 250 pmol of RGFP966 before adding acetonitrile. Supernatants were dried by vacuum centrifugation and resolubilized by adding 50 μL water containing 40% (v/v) acetonitrile, 0.1% (v/v) formic acid, and incubating in a sonicating bath for 30 min. Samples were then centrifuged 5 min at 16,000 *g* and 25 μL transferred to an autosampler vial for 20 μL injection. Online high performance liquid chromatography (HPLC) was performed using an Agilent 1100 HPLC system (Agilent Technologies, Santa Clara, CA), with capillary pump, column compartment, and micro well-plate autosampler. The capillary pump was operated in normal (as opposed to capillary) mode. Solvents were 0.1% (v/v) formic acid in water and 0.1% (v/v) formic acid in acetonitrile. The column was a Phenomenex Kinetex C18, 2.0×50 mm column with 2.6 μm particles (Phenomenex, Torrance, CA). The flow rate as 250 μL/min with gradient elution starting at 5% formic acid in acetonitrile during sample loading, hold for 2 min, then progressing linearly to 95% formic acid in acetonitrile at 20 min, hold for 1 min, and return to 5% formic acid in acetonitrile over 1 min with a re-equilibration for a further 15 min at 5% formic acid in acetonitrile. The column was held at 30°C during loading and elution. The autosampler was held at 5°C. RGFP966 eluted at 14 min. Mass spectrometry was performed using a Sciex 3200 QTRAP system with TurboIon V source (Framingham, MA). Source parameters for liquid chromatography and tandem mass spectroscopy (LC-MS/MS) were: CUR = 30; CAD gas = high; IS = 4500 V; TEM = 650C; GS1 = 50; GS2 = 30; DP = 10 V; EP = 10 V; CXP = 10 V. Data were acquired in selected reaction monitoring mode using Q1–Q3 transitions previously optimized for RGFP966 by direct infusion of the drug. Two transitions were monitored: m/z 363.1–m/z 237.1 at collision energy (CE) of 23 V, and m/z 363.1–m/z 117.1 at CE 30 V. The dwell time for each transition was 150 ms. Data from the m/z 363.1–237.1 transitions were used for quantitation, whereas the m/z 363.1–m/z 117.1 transition was used for confirmation. Transition chromatograms were smoothed twice and peak areas calculated for calibrants and samples. Concentrations were determined by linear fit through zero using the Analyst 1.4.2 software (Sciex).

Statistical analyses

Data were collected from a minimum of 4 independent mice in all experiments, except for analysis of heterochromatin formation ($n=3$) and mass spectrometry ($n=3$). For cell counts in whole mounts, data were collected from twenty-four 100 μm^2 regions from each retina. The mean was therefore determined between 96 and 120 regions per treatment group, and data were shown as the mean ± standard error. Data from intestinal BrdU counts and retinal heterochromatin scoring from images of sections were also represented by the mean and standard error within each treatment group. All statistical analyses were performed using the Student's *t*-test with statistical significance set to $P=0.05$.

Results

Single intravitreal injection of HDAC3-specific inhibitor RGFP966 prevents histone deacetylation in a dose-dependent manner following ONC

Peak histone deacetylation in RGCs occurs at 5 days following ONC, and this event occurs concurrently with HDAC3 translocation to the nucleus.[3] Importantly, histone deacetylation is ameliorated in RGCs, where *Hdac3* is conditionally knocked out in these cells, indicating a critical role for HDAC3 activity in the deacetylation event.[8] Selective inhibition of HDAC3 in the retina by an intravitreal injection of RGFP966 was assessed by counting AcH4-positive cells in the GCL 5 days after ONC. Eyes were treated with either HPβCD vehicle or increasing doses (1.0, 2.0, 7.0, and 10.0 μM) of RGFP966 immediately following ONC (Fig. 1A–E). Results indicated a dose-dependent response in histone H4 acetylation. Approximately 30% of the cells in the GCL of vehicle-treated eyes exhibited widespread deacetylation of histone H4. This effect was reduced with increasing concentrations of injected RGFP966, with the significant peak response occurring in the 2 μM treatment group compared with injured control and treated retinas ($P<0.0001$) (Fig. 1E). Suppression of histone deacetylation was less effective with concentrations of drug greater than 2 μM ($P<0.003$). Therefore, for the remaining experiments assessing the nuclear atrophic events following acute optic nerve damage, we designated the HPβCD vehicle and the 10 μM RGFP966-treated eyes as negative and high-dose controls, respectively (Figs. 1B and 2D), the untreated uninjured contralateral eyes as healthy controls (Fig. 1A), and the 2 μM RGFP966-treated eyes as the experimental treatment group (Fig. 1C).

Single intravitreal injection of 2 μM RGFP966 ameliorates heterochromatin formation in RGCs following ONC

Conditional knockout of *Hdac3* expression in RGCs before ONC led to protection against heterochromatin formation and nuclear condensation.[8] Here, intravitreal injection of 2 μM RGFP966 immediately following ONC also prevented heterochromatin formation in the nucleus 5 days after axonal injury (Fig. 2A–D). Masked cell scoring of the GCL in retinal sections 5 days after ONC demonstrated that retinas treated with 2 μM RGFP966 had significantly more euchromatic cells and fewer heterochromatic and pyknotic cells when compared with the HPβCD vehicle and 10 μM RGFP966-treated retinas ($P<0.0001$) (Fig. 2E–I).

Single intravitreal injection of 2 μM RGFP966 reduces apoptosis and DNA damage in RGCs up to 7 days after ONC

Late hallmark events of the apoptotic pathway include nuclear condensation, DNA damage and nuclear fragmentation,

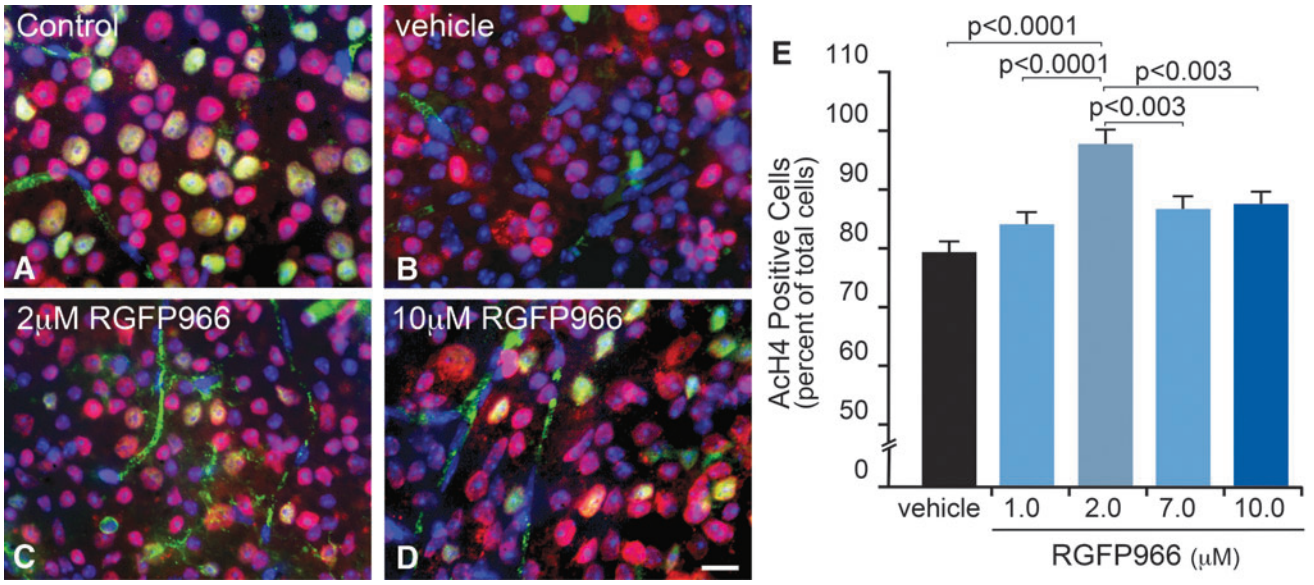

FIG. 1. Intravitreal injection of RGFP966 prevents histone H4 deacetylation when administered at a 2.0 μM concentration to the vitreous. Mice were injected intravitreally with 30% HPβCD, 0.1 M acetate (pH 5.4) vehicle, 1.0, 2.0, 7.0, or 10.0 μM RGFP966 immediately following ONC surgery. Five days later, retinas were whole mounted and fluorescently labeled for AcH4 (Texas Red), BRN3A (Alexa-488), and DNA with DAPI. **(A)** Uninjured untreated control OD retinas contained healthy, BRN3A (*green*), and AcH4 (*red*) positively labeled cells in the GCL. Note that blood vessels in the GCL are nonspecifically labeled by the BRN3A antibody. **(B)** OS retinas that were treated with vehicle showed a reduction in AcH4 positively labeled cells and exhibited a visible loss of expression of BRN3A, which is consistent with previous evidence that RGC-specific gene silencing occurs shortly after ONC.[2] **(C, D)** OS retinas that were treated with 2.0 or 10.0 μM RGFP966 retained more AcH4 and BRN3A-positive cells than vehicle-injected retinas following ONC. Scale bar = 10 μm. **(E)** Cell counts for the dose–response curve indicated that significant abolition of the histone deacetylation response resulted from single treatment with an HDAC3-specific inhibitor immediately following ONC, with the highest percentage of AcH4-positive cells present in the 2.0 μM treatment paradigm ($P < 0.0001$, relative to vehicle and 1.0 μM; $P < 0.003$, relative to 7.0 and 10.0 μM). AcH4, acetylated histone 4; BRN3A, brain-specific homeobox/POU domain protein 3A; DAPI, 4′, 6-diamidino-2-phenylindole; GCL, ganglion cell layer; HPβCD, 2-hydroxypropyl-beta-cyclodextrin; ONC, optic nerve crush.

and subsequent cell removal. These events were monitored at 5, 7, and 14 days after ONC, respectively, in RGFP966-treated and control mice. At 5 days after ONC, neuron-specific nuclear condensation in the GCL of whole-mounted retinas was assessed by immunofluorescence staining for the RGC-selective marker beta-III tubulin (TUJ-1).[17] The retinas of mice treated intravitreally with HPβCD vehicle or 10 μM RGFP966 (Fig. 3B, D) had visibly more TUJ-1-positive cells with condensed or fragmented nuclei in the GCL in comparison to uncrushed control or 2 μM RGFP966-treated retinas (Fig. 3A, C). Quantification of TUJ-1-positive apoptotic cells in the GCL confirmed that HPβCD vehicle-treated eyes had a significantly higher percentage of apoptotic TUJ-1-positive cells than the 2.0 and 10.0 μM RGFP966-treated eyes ($P < 0.0001$), whereas 2.0 μM RGFP966 provided significantly more protection than 10.0 μM RGFP966 ($P = 0.0001$) (Fig. 3I).

Seven days after ONC, retinas were harvested, whole mounted, and labeled for DNA fragmentation using TUNEL. Control OD retinas that were left uncrushed and untreated, exhibited sparse labeling with TUNEL, whereas over 10% of cells in the GCL labeled positive for TUNEL in OS retinas that were crushed and treated with HPβCD vehicle (Fig. 3E, F). Retinas that were treated with 2.0 and 10.0 μM RGFP966 contained some TUNEL-positive cells, indicating that low levels of DNA fragmentation had occurred (Fig. 3G, H), but this was significantly less than the HPβCD vehicle-injected OS eyes ($P < 0.0001$). As with the presence of apoptotic TUJ-1 cells, 2.0 μM RGFP966 provided significantly more protection against DNA damage in comparison to 10.0 μM RGFP966 ($P < 0.0001$) (Fig. 3J).

We also evaluated the percentage of cells that still expressed the RGC-specific transcription factor BRN3A at 14 days after ONC. BRN3A mRNA levels are rapidly depleted in damaged RGCs[18] although protein levels have been reported to persist for several days.[19] Significant protection against BRN3A-positive cell loss was achieved in 2.0 μM RGFP966 intravitreally injected OS eyes when compared with HPβCD vehicle-injected OS eyes ($P < 0.0001$) (Fig. 3K). While this protective effect was significant, treated retinas still showed upward of 80% loss of expressing cells. In addition, total cell loss was not ameliorated (data not shown). These data indicated that a single dose of RGFP966 yielded only a transient effect, necessitating repeated or systemic dosing to achieve a long-lasting effect such as might be expected to be protective in a chronic disease such as glaucoma.

Systemic administration of 10 mg/kg RGFP966 daily for 14 days does not elicit gross toxicity in other bodily tissues and does not affect mucosal cell proliferation in the small intestine

HDAC inhibitors can induce cell cycle arrest and/or apoptosis of dividing cells.[20] Therefore, to test whether repeated systemic application of RGFP966 elicited toxic

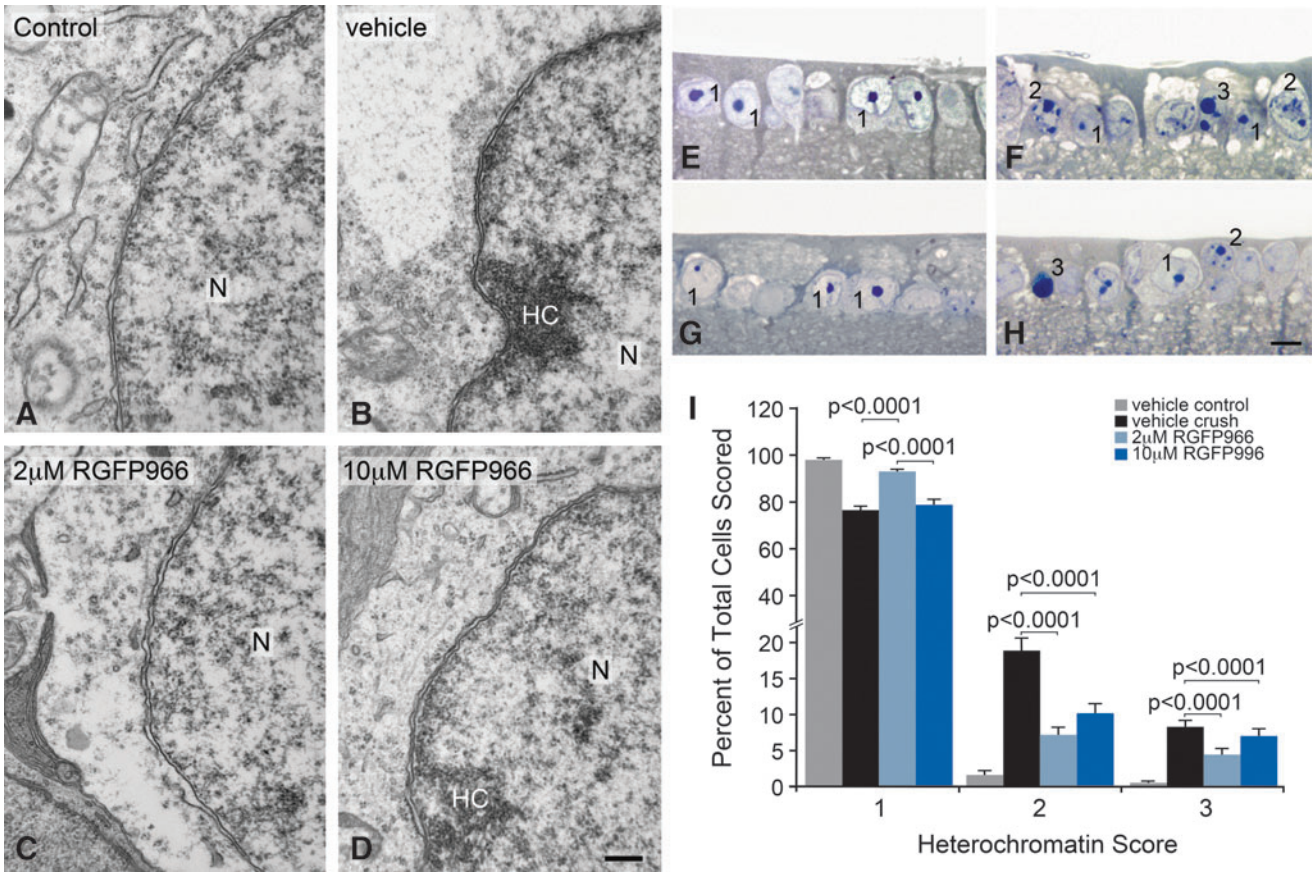

FIG. 2. Intravitreal injection of 2.0 μM RGFP966 prevented chromatin condensation at 5 days following ONC. Intravitreal injection of HPβCD vehicle, 2.0 or 10.0 μM RGFP966 was administered immediately following ONC. Eyes were harvested at 5 days following ONC, and cells in the GCL were imaged using TEM. **(A)** Uninjured and untreated retinas contained predominantly euchromatic nuclei in the GCL with well-formed nuclear membranes. **(B)** HC formation in the N accumulated along the double membrane of the nuclear envelope in vehicle-injected eyes that underwent axonal injury from ONC. **(C)** Retinas treated with 2.0 μM RGFP966 had less heterochromatin accumulation at the nuclear envelope than vehicle-treated retinas and maintained intact nuclear membranes and pores. **(D)** Dosing with 10.0 μM RGFP966, however, did not protect cells in the GCL from heterochromatin accumulation in the nucleus. Scale bar = 300 nm. Retinas were harvested at 5 days following ONC, retinal tissue was sectioned from plastic mounting and stained with Methylene Blue and Azure Blue stain, and cells were scored for level of chromatin condensation by masked observation from bright-field imaging of the GCL. **(E)** Uninjured and untreated OD retinas had round, healthy-appearing nuclei in the GCL. **(F)** Retinas that underwent ONC and received a single HPβCD vehicle injection contained cells in the GCL with partial apoptotic heterochromatin formation and cells that were completely heterochromatic. **(G)** The intravitreal treatment with 2.0 μM RGFP966 resulted in more healthy-appearing nuclei in the GCL than in the retinas that were treated with 10.0 μM RGFP966 or HPβCD vehicle. **(H)** Retinas treated with 10.0 μM RGFP966 had visibly more cells that were partially and completely heterochromatic in the GCL. Scale bar = 10 μm. **(I)** Masked cell counts indicated that retinas with 2.0 μM RGFP966 treatment after ONC had significantly more cells with a score of 1 in the GCL, indicating a normal euchromatic appearance of the nucleus, when compared with vehicle and 10.0 μM RGFP966-injected retinas ($P < 0.0001$ and $P < 0.0001$, respectively), whereas there was no significant difference between vehicle crush and 10.0 μM treated eyes ($P > 0.05$). Treating eyes with 2.0 or 10.0 μM RGFP966 significantly reduced the number of cells showing partial heterochromatin formation (score of 2) compared with vehicle-treated crush eyes ($P < 0.0001$ for 2.0 μM and $P < 0.0001$ for 10.0 μM). There was no significant difference between scores for 2.0 and 10.0 μM. Similarly, RGFP966 reduced the overall number of pyknotic cells (score of 3) compared with vehicle-treated crush eyes ($P < 0.0001$ for 2.0 μM and $P < 0.0001$ for 10.0 μM), while showing no significant difference between the 2 RGFP966 treatment groups. Heterochromatin score of 1 = healthy cell with euchromatic nucleus and well-formed nucleolus, 2 = cell with partial apoptotic heterochromatin formation, and 3 = cell with completely heterochromatic (pyknotic) nucleus. HC, heterochromatin; TEM, transmission electron microscopy; N, nucleus.

effects to tissues that normally require cell division, mice were injected IP with HPβCD vehicle or 10 mg/kg RGFP966 every day for 14 days. The tissues of heart, small intestine, kidney, liver, lung, and skin were then harvested, processed for paraffin embedding, sectioned, and stained with H&E stain. Sections were then qualitatively analyzed by a veterinary pathologist. Pathological read-out of H&E-stained sections of tissues suggested no evidence of toxic side effects in these organs (Fig. 4) or in regions of the central nervous system (Fig. 5), including no immune cell infiltration or abnormal cellular morphology (Fig. 5A–L). To further quantify any effects on cell division, mice were also

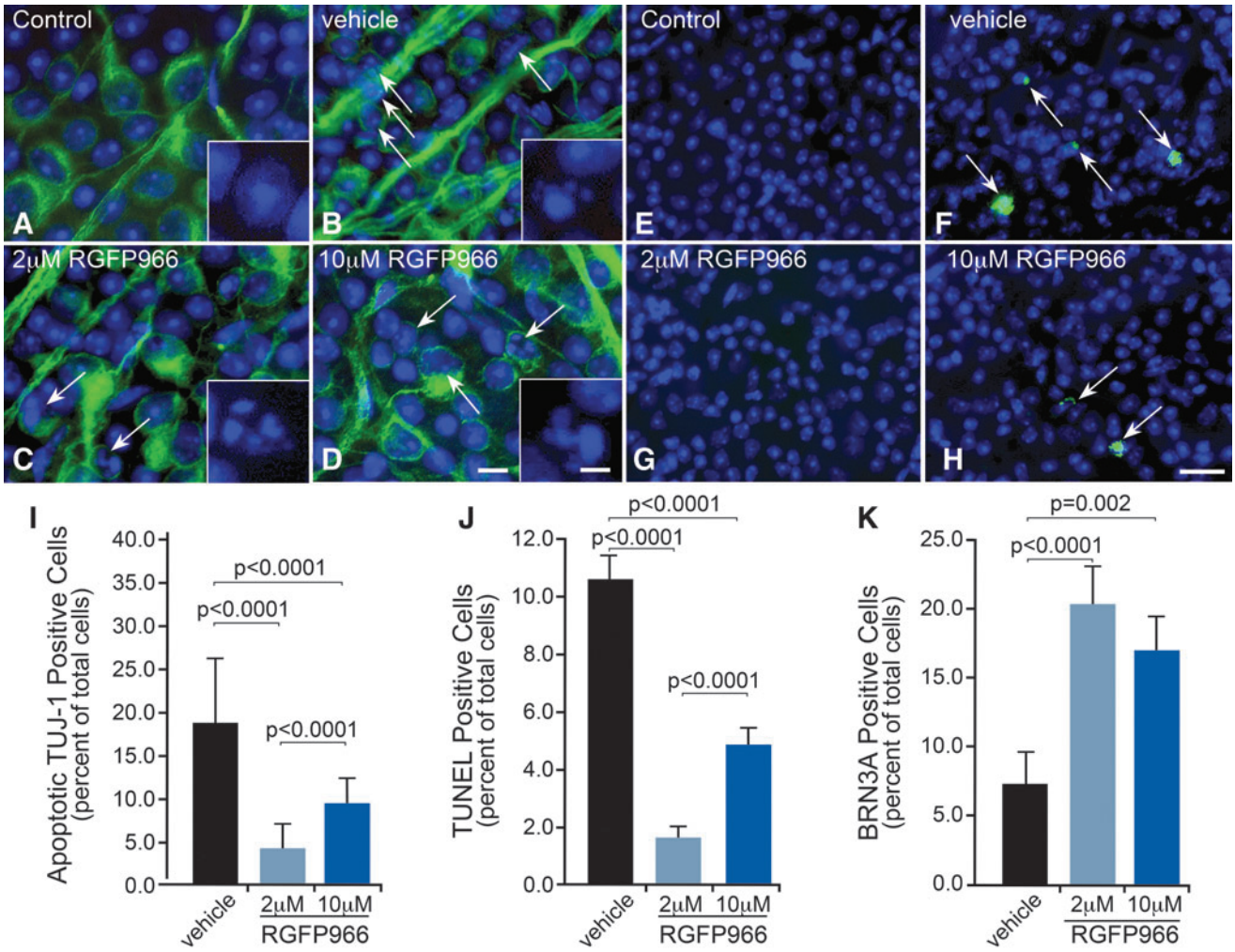

FIG. 3. RGC apoptosis and DNA damage were ameliorated following ONC with a single intravitreal injection of 2 μM RGFP966. Retinal whole mounts were harvested at 5 days post ONC, antibody labeled for neurons in the GCL using TUJ-1 (Alexa-488), and labeled for nuclei using DAPI. **(A)** Immunofluorescence imaging revealed no neurons in the GCL that underwent apoptosis in the control uncrushed and untreated OD eyes. The *inset* shows a higher magnification example of a typical normal-appearing nucleus of cells that are designated as neurons (DAPI stain only). **(B)** In the vehicle-injected OS eyes that underwent ONC, several neuronal cells in the GCL exhibited condensed DAPI-stained nuclei at 5 days postinjury. **(C, D)** Treatment with RGFP966 prevented neuronal apoptosis in the GCL when dosed at 2.0 and 10.0 μM immediately following ONC. The *insets* in **(B–D)** show examples of nuclei designated as undergoing apoptosis. Scale bar = 10 μm (5 μm in *insets*). **(E)** Control OD retinas that were left uncrushed and untreated exhibited sparse labeling with TUNEL, whereas **(F)** over 10% of cells in the GCL labeled positive for TUNEL in OS retinas that were crushed and treated with vehicle. *Arrows* mark TUNEL-positive cells that were scored in this image, which included cells with initial signs of DNA fragmentation and cells with extensive DNA fragmentation. **(G, H)** Retinas that were treated with 2.0 and 10.0 μM RGFP966 contained some TUNEL-positive cells, indicating that low levels of DNA fragmentation had occurred. *Arrows* in **(H)** indicate TUNEL-positive cells that were scored in this image. Scale bar = 50 μm. **(I)** Cell counts of TUJ-1 positive apoptotic cells in the GCL indicated that HPβCD vehicle-treated eyes had a significantly higher percentage of apoptotic TUJ-1-positive cells than the 2.0 μM and 10.0 μM RGFP966-treated eyes ($P < 0.0001$ for 2.0 μM and $P < 0.0001$ for 10.0 μM). Also, treatment with 2.0 μM RGFP966 provided significantly more protection from neuronal apoptosis than treatment with 10.0 μM RGFP966 ($P < 0.0001$). At 7 days postcrush, retinas were harvested, whole mounted, and labeled for DNA fragmentation using TUNEL. **(J)** HPβCD vehicle-injected OS eyes had significantly more cells exhibiting DNA fragmentation when compared with 2.0 and 10.0 μM RGFP966-injected OS eyes ($P < 0.0001$ for 2.0 μM and $P < 0.0001$ for 10.0 μM). The 2.0 μM RGFP966 injection immediately after ONC provided significantly more protection against DNA damage in comparison to 10.0 μM RGFP966 injection ($P < 0.0001$). **(K)** At 14 days postcrush, retinas were harvested, whole mounted, and labeled for BRN3A and DAPI for cell counts. The 2.0 and 10.0 μM RGFP966 injection similarly attenuated the loss of BRN3A-positive cells in the GCL, which was significant when compared with vehicle-injected eyes ($P < 0.0001$ and $P = 0.002$, respectively). TUJ-1, beta-III tubulin.

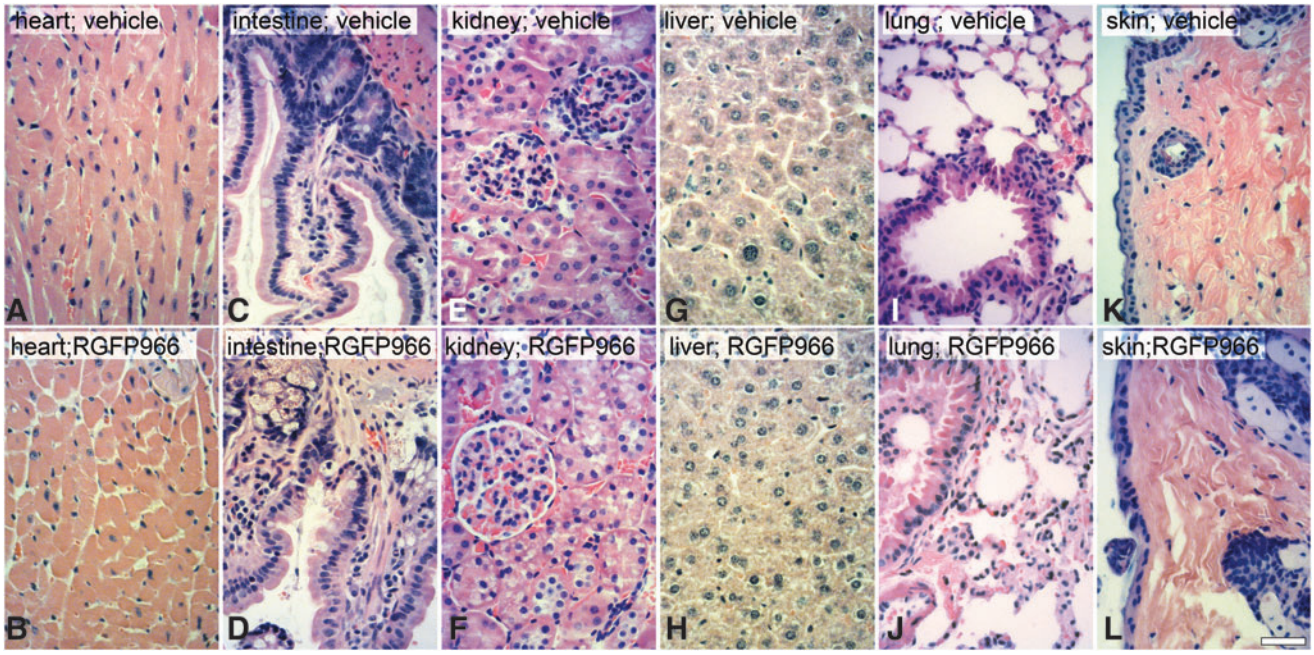

FIG. 4. Systemic injection of 10 mg/kg RGFP966 daily for 14 days does not induce gross toxicity to major organs. Mice were injected IP with 30% HPβCD 0.1 M acetate (pH 5.4) vehicle, 2 mg/kg RGFP966 (data not shown), or 10 mg/kg RGFP966 every day for 14 days. The **(A, B)** heart, **(C, D)** small intestine, **(E, F)** kidney, **(G, H)** liver, **(I, J)** lung, and **(K, L)** skin were then harvested, processed for paraffin embedding, sectioned, and stained with H&E stain. The pathology results describe no vacuolization, nuclear fragmentation, polymorphonuclear or other immune cell infiltration, abnormal morphology, structural disorder, or indication of a toxic environment in any of the RGFP966-treated mice when compared with vehicle-treated mice. Scale bar = 10 μm. IP, intraperitoneal.

injected IP with 2 mg of BrdU at 24 h before euthanasia. The small intestine immediately inferior to the duodenum was then harvested, processed, and immunostained for BrdU incorporation. The results from the BrdU cell counts indicated that both HPβCD vehicle and RGFP966-treated mice had normal intestinal mucosa with similar numbers of BrdU-positive mucosal cells in S-phase in the crypts (Fig. 6A–C). Lastly, mice treated with RGFP966 showed no significant change in weight over vehicle-treated mice during the 14-day period (Fig. 6D).

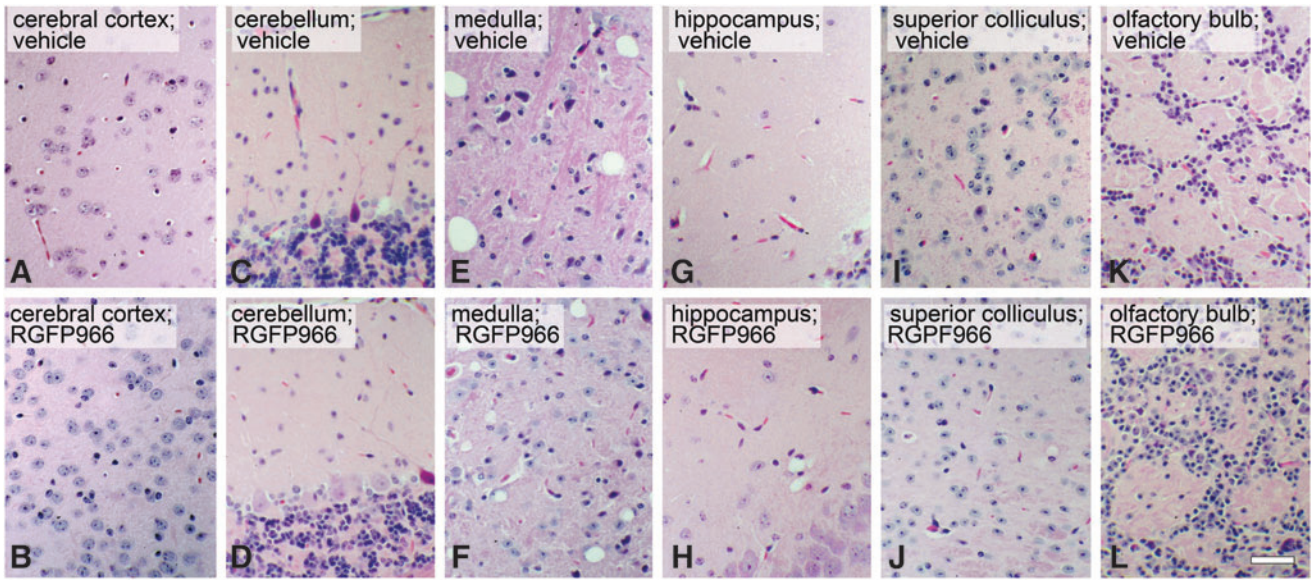

FIG. 5. Systemic injection of 10 mg/kg RGFP966 daily for 14 days does not induce gross toxicity to the brain. Mice were injected IP with 30% HPβCD 0.1 M acetate (pH 5.4) vehicle, 2 mg/kg RGFP966 (data not shown), or 10 mg/kg RGFP966 every day for 14 days. The brain was then harvested, processed, and stained with H&E stain. **(A–L)** Sagittal sections were then analyzed by a veterinary pathologist. The pathology results described no vacuolization, nuclear fragmentation, polymorphonuclear or other immune cell infiltration, abnormal cellular morphology besides artifact of processing, structural disorder, or indication of toxic environment in any of the RGFP966-treated mice when compared with vehicle-treated mice. Scale bar = 10 μm.

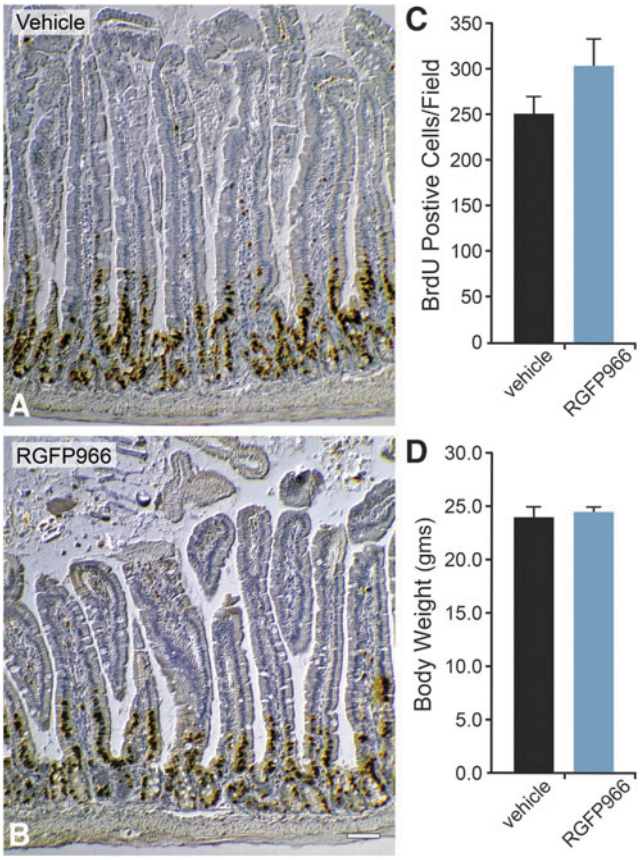

FIG. 6. Systemic injection of 10 mg/kg RGFP966 daily for 14 days does not affect mucosal cell proliferation in the small intestine. Mice were injected IP with 30% HPβCD 0.1 M acetate (pH 5.4) vehicle **(A)** or 10 mg/kg RGFP966 **(B)** daily for 14 days. Mice were injected IP with 2 mg of BrdU at 24 h before euthanasia. The small intestine inferior to the duodenum was then harvested, processed, and immunostained for BrdU. The total number of cells labeled positive for BrdU in each image was then analyzed using ImageJ/Fiji particle analysis counting software. **(C)** The total number of BrdU-positive mucosal cells in the vehicle-treated mouse intestinal sections was not significantly different from that of the RGFP966-treated mouse intestinal sections. Scale bar = 20 μm. **(D)** Body weights were taken before and after 14 days of RGFP966 treatment, and the average body weights showed no significant change ($P > 0.05$).

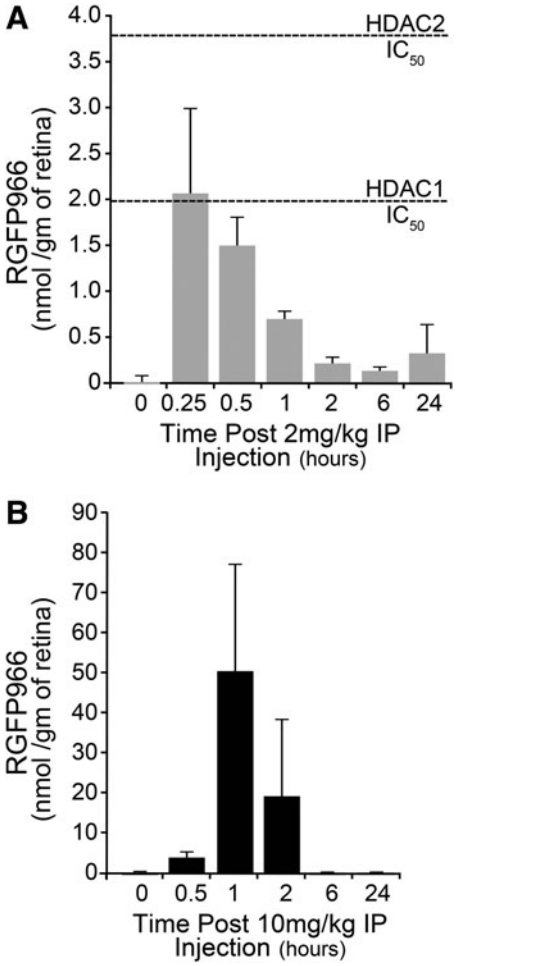

FIG. 7. Concentration of RGFP966 in the retina after systemic injection. Mass spectrometry was used to investigate localization of RGFP966 to the mouse retina after IP injection. **(A, B)** IP injection of 2 or 10 mg/kg RGFP966 was followed by euthanasia and retinal harvest at 0, 0.5, 1, 2, 6, and 24 h postinjection. Retinas were then analyzed using MS/LC to determine the concentration of RGFP966 in nmol/g of retinal tissue. The maximum drug concentration (C_{max}) in the retina occurred 15 min after the 2 mg/kg injection and 1 h after the 10 mg/kg injection. The IC_{50} value for HDAC3 on this scale is 0.06 nmol/g retina. The IC_{50} values for HDAC1 and HDAC2, respectively, are shown by *hashed lines* in **(A)**. MS/LC, mass spectrometry and liquid chromatography.

RGFP966 bioavailability in the retina after IP injection

RGFP966 is known to cross the blood–brain barrier and has been used as a therapeutic for cocaine-seeking behavior in mice.[12] Before using RGFP966 as a systemic therapeutic to prevent RGC death post ONC, we first investigated the bioavailability time course of RGFP966 to the mouse retina after IP injection by using mass spectrometry. In mice injected with 2 mg/kg RGFP966, the maximum drug concentration (C_{max}) in the retina occurred after 15 min when it reached 2.3 nmol/g to achieve 1.97 μM in the retina (Fig. 7A). This value falls within the appropriate range for selective inhibition of HDAC3 and potentially HDAC1 (Fig. 7A and Table 1). After 15 min, the concentration of RGFP966 in the retina dropped to a range for selective inhibition of HDAC3. In the retinas of mice injected with 10 mg/kg RGFP966, the bioavailability peaked 1 h after injection, at 52.55 nmol/g retina (Fig. 7B), or equivalent to a concentration of 52.55 μM. This concentration exceeded the IC_{50} values for HDACs 1, 2, and 3. In each time course, the RGFP966 was cleared from the retina after 2 h and was virtually undetectable in the retina 24 h post IP injection.

Systemic RGFP966 treatment prevents histone deacetylation in a dose-dependent manner following ONC

To test if systemic injection of RGFP966 prevented histone deacetylation at 5 days post ONC, control mice were either

left uninjected or were injected IP with HPβCD vehicle; whereas dosed mice were injected with 2, 6, or 10 mg/kg RGFP966 immediately following ONC. Whole mounts were then labeled for AcH4 and DAPI for cell counts. Uninjured control OD retinas contained healthy AcH4 positively labeled cells in the GCL, whereas OS retinas of mice that received no injection or vehicle injection showed a reduction in the percentage of AcH4 positively labeled cells (Fig. 8A–C). OS retinas of mice that were treated with 2, 6, or 10 mg/kg RGFP966 retained more AcH4-positive cells than untreated or vehicle-treated mice following ONC (Fig. 8D–F). Cell counts for the dose–response curve indicated that significant retention of histone acetylation resulted from a single treatment with RGFP966 immediately following ONC in all treated animals ($P < 0.0001$) (Fig. 8G).

Systemic injection of 2 mg/kg RGFP966 every 3 days provides long-term attenuation of histone deacetylation and prolongs cell survival in the GCL

To determine whether extended RGFP966 treatment in a specific dose could provide maximal inhibition of histone deacetylation, while conferring prolonged protection to cells in the GCL, mice were either injected IP with vehicle, 2, or 10 mg/kg RGFP966 every day, every 3 days, or every 7 days following ONC. Fourteen days after ONC, retinas were harvested, whole mounted, and stained with DAPI for counting cells. Retinas from mice that were treated with 2 mg/kg RGFP966 every 3 days maintained significantly more DAPI-positive cells when compared with vehicle-treated animals ($P < 0.0001$) as well as when compared with daily ($P < 0.0001$) and weekly treatments ($P < 0.0001$) with 2 mg/kg RGFP966 (Fig. 9A). Consistent with this overall protective effect, the same treatment paradigm of 2 mg/kg RGFP966 injected every 3 days also provided the greatest attenuation of histone H4 deacetylation in comparison to other treatment groups ($P = 0.0002$, $P < 0.0001$, and $P = 0.004$, respectively) (Fig. 9B).

Using the treatment paradigm of injecting every 3 days with vehicle, 2, or 10 mg/kg RGFP966, retinas were harvested at 14 and 28 days post ONC to interrogate the effect of treatment on BRN3A expression and total cell numbers in the GCL. Retinas of mice that were treated with 2 or 10 mg/kg RGFP966 every 3 days maintained significantly more BRN3A positive when compared with vehicle-treated mice at 2 weeks post ONC ($P = 0.002$ and $P < 0.0001$, respectively) (Fig. 10A). The protective effect on gene expression was transient; however, since by 4 weeks, treatment with either 2 or 10 mg/kg RGFP966 failed to preserve the BRN3A expression (Fig. 10B). Conversely, the overall cell loss at 4 weeks post ONC was significantly inhibited by injections of 2 mg/kg RGFP966 in comparison to vehicle and 10 mg/kg RGFP966 ($P < 0.0001$) (Fig. 10C).

Discussion

Nuclear atrophy is an early response to axonal damage in RGCs, and it is characterized by histone deacetylation, heterochromatin formation, and gene silencing. HDACs 1, 2, and 3 are known to play important roles in this early response, and interestingly, HDAC3 translocates to the nuclei of RGCs in concert with histone deacetylation.[3] Importantly, conditional knockout of *Hdac3* in RGCs, before ONC, was found to protect against histone deacetylation, global heterochromatin formation, and apoptosis of these cells.[8] While ablation of *Hdac3* provided proof of a role for this enzyme, demonstrating similar effects using an HDAC3 inhibitor is an important step in translating these findings to a therapeutic application. Therefore, we sought to investigate the effects of an HDAC3 selective inhibitor, RGFP966, in the same acute model of RGC death.

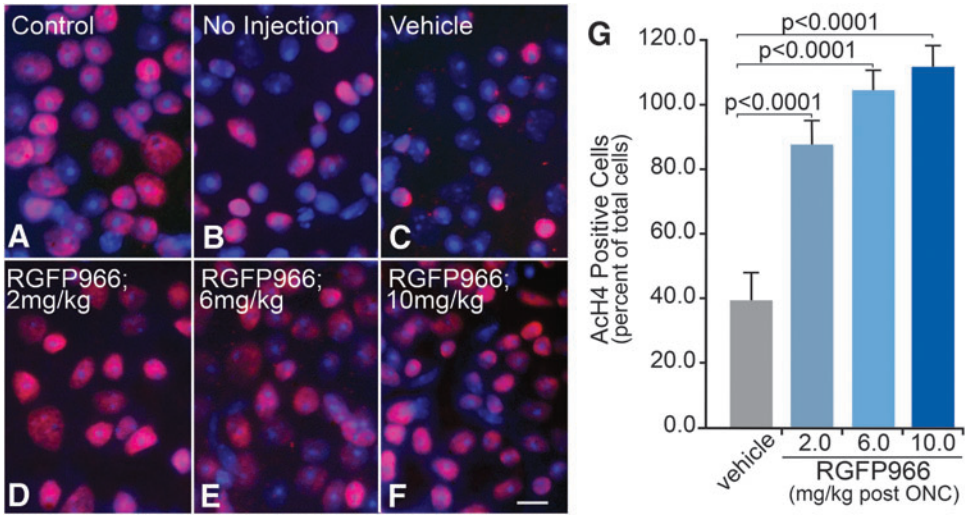

FIG. 8. Systemic injection of RGFP966 prevents histone H4 deacetylation when administered at 2, 6, and 10 mg/kg doses immediately after ONC. Mice were IP injected with 2–10 mg/kg RGFP966, and 5 days later, retinas were harvested, whole mounted, and stained for AcH4 and DAPI to count cells. **(A)** Uninjured control OD retinas contained healthy AcH4 positively labeled cells in the GCL. **(B, C)** OS retinas of mice that received no injection or vehicle injection showed a reduction in AcH4 positively labeled cells. **(D–F)** OS retinas of mice that were treated with 2, 6, or 10 mg/kg RGFP966 retained more AcH4-positive cells than untreated or vehicle-treated mice following ONC. **(G)** Cell counts show that all RGFP966-treated animals maintained significantly more cells that were positive for AcH4 when compared with the vehicle control ($P < 0.0001$). Scale bar = 10 μm.

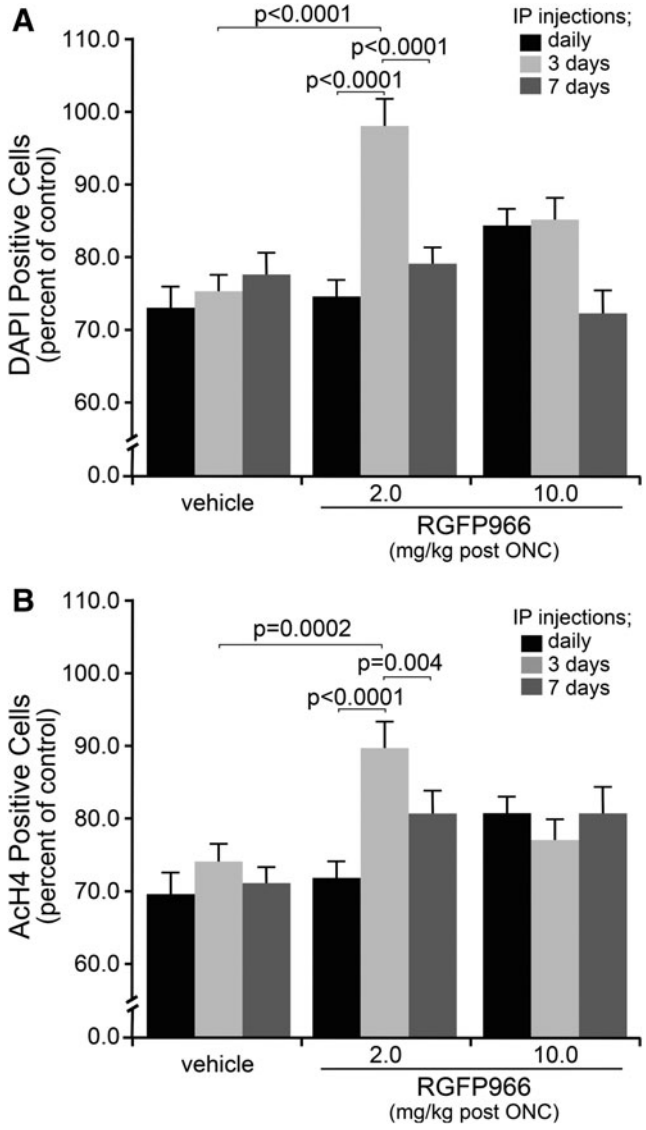

FIG. 9. Systemic injection of 2 mg/kg RGFP966 every 3 days results in the retention of total cells in the GCL at 14 days following ONC. Mice were either injected IP with 30% HPβCD 0.1 M acetate (pH 5.4) vehicle, 2, or 10 mg/kg RGFP966 daily, every 3 days, or every 7 days following ONC. Fourteen days after ONC, retinas were harvested, whole mounted, and stained for AcH4 and DAPI for counting cells. **(A)** An estimate of total cells in the GCL remaining in crushed eyes, based on DAPI staining, shows that 2 mg/kg injections every 3 days provide significant protection over vehicle injections ($P < 0.0001$) and over every day ($P < 0.0001$) and every 7 day ($P < 0.0001$) injections of the same concentration of RGFP966. None of the injection paradigms for 10 mg/kg RGFP966 provided a significant protective effect for cell loss. **(B)** Results from AcH4-positive cell counts indicate a significant retention of total cells and acetylation of histone H4 in the GCL of retinas from mice treated with 2 mg/kg RGFP966 every 3 days following ONC in comparison to vehicle every 3 days ($P = 0.0002$), 2 mg/kg daily ($P < 0.0001$), and 2 mg/kg weekly ($P = 0.004$).

Here, we found that a single intravitreal injection of RGFP966 immediately after ONC elicited protection against nuclear atrophy, similar to the *Hdac3* conditional knockout. However, the protective effect from the single intravitreal treatment was transient, likely the result of clearance of the small molecule drug from the vitreous[21] and the need to have more sustained protection.

There are benefits and caveats with the current methods of drug administration to treat retinal dysfunction. Intravitreal injections are used to deliver drugs effectively to the retina, and are currently the standard of practice for the treatment of neovascular age-related macular degeneration.[21] These injections are invasive, however, and can cause adverse effects, such as endophthalmitis and retinal detachment, if patients are repeatedly treated in this manner.[22] An alternative approach, such as placing a local slow-release intraocular implant, may be a viable option to provide a long-acting therapy for glaucoma patients; however, the same caveats with infection and retinal detachment are also factors.[22]

Systemic application using drugs, which can penetrate the blood–retinal barrier, can be used to reach the retina, however, a small fraction of the drug can reach the retina from the blood stream, making it necessary to deliver high doses of drug systemically to achieve adequate bioavailability in the retina.[23] Prolonged administration of high doses of broad-spectrum HDAC inhibitors may damage both on-target and off-target cell types, particularly gastrointestinal cells, immune cells, and cardiac cells. The results of these effects have been seen in human trials, where the common side effects are fatigue, thrombocytopenia, gastrointestinal toxicity, and prolongation between the Q and T waves of an electrocardiogram.[24] Treating with HDAC isotype inhibitors may avoid the toxic effects of off-target binding, however, further investigation is needed to determine proper dosing for safe and effective treatment.[25] Therefore, a range of concentrations of RGFP966 was tested systemically to confirm both the bioavailability of the drug in the retina at therapeutic levels that affects biological indicators, or metrics, of RGC nuclear atrophy and apoptosis after ONC.

Changing the concentration of intravitreal or systemic RGFP966 led to differential effects on metrics of RGC health and survival long after ONC, which was likely a result of bioavailability of RGFP966 in the retina. Systemic injection of 2 mg/kg yielded a 25-fold decrease in maximal concentration in the retina when compared with 10 mg/kg dosing, a phenomenon, which may be a result of differential rates of absorption and binding of the drug to systemic targets before RGFP966 crossing the blood–retina barrier. At low levels, which selectively inhibit HDAC3, effects on global histone deacetylation and RGC survival were maximized. At higher levels, however, which reached concentrations that could influence the activity of HDACs 1 and 2, but are less effective at inhibiting HDAC3, RGFP966 was able to attenuate the decrease in BRN3A expression at 2 weeks post ONC, but was less effective at preventing RGC loss long term.

Normally *Brn3a* expression is shutdown after damage,[18] an effect that is common to multiple RGC-specific genes. Importantly, the silencing of normal RGC-specific gene expression can be dissociated from the commitment of RGCs to the apoptotic pathway. Gene expression silencing, for example, still occurs in *Bax*-deficient RGCs,[2,7,26] even though the apoptotic program is essentially permanently blocked.[27] The effect of higher concentrations of RGFP966 on transcriptional silencing, although transient, suggests a potentially important role for HDACs 1 and 2 in maintaining RGC-specific gene expression after axonal injury. This result partially mimics the effect of trichostatin A, a broad-spectrum class I HDAC inhibitor, on preventing gene silencing in injured RGCs.[3,7]

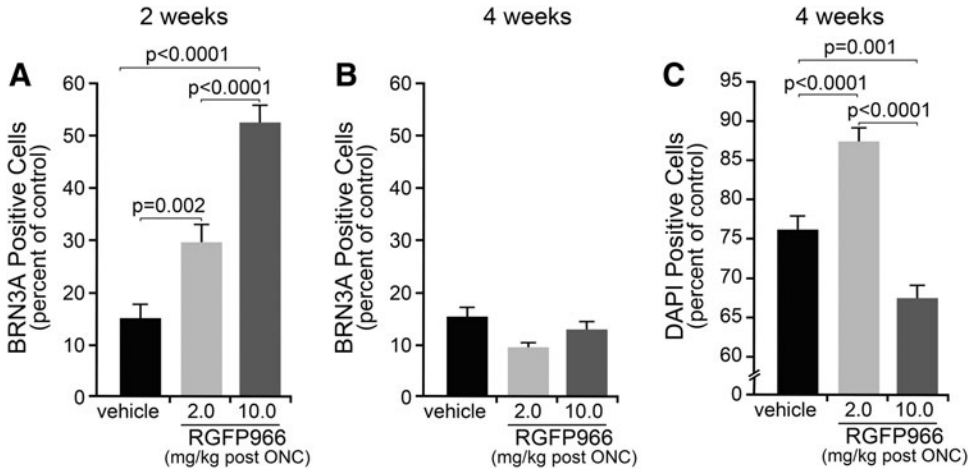

FIG. 10. Systemic injection of 2 mg/kg RGFP966 every 3 days results in protection against BRN3A expression loss at 2 weeks post ONC and total cell loss at 4 weeks post ONC. Mice were either injected IP with 30% HPβCD 0.1 M acetate (pH 5.4) vehicle, 2, or 10 mg/kg RGFP966 every 3 days following ONC. Fourteen and 28 days after ONC, retinas were harvested, whole mounted, and stained for BRN3A and DAPI for counting cells. **(A)** At 2 weeks post ONC, experimental retinas from eyes of mice IP injected with vehicle contained significantly fewer BRN3A-labeled cells than in 2 or 10 mg/kg RGFP966-treated mice ($P = 0.002$ and $P < 0.0001$, respectively). IP injection of 10 mg/kg provided significantly more protection against loss of BRN3A expression than 2 mg/kg treated mice ($P < 0.0001$). **(B)** By 4 weeks post ONC, however, IP injection of RGFP966 at either concentration failed to prevent the loss of BRN3A. **(C)** Total cell counts based on DAPI labeling indicated a significant attenuation of cell loss in 2 mg/kg treated eyes over eyes in mice IP injected with vehicle or 10 mg/kg ($P = 0.002$ and $P < 0.0001$, respectively). Greater cell loss relative to vehicle-treated mice was detected in 10 mg/kg treated animals ($P = 0.001$).

Both HDAC-dependent events appear to be important for RGC survival, although to different levels of efficacy. Historically, broad-spectrum HDAC inhibition has been shown to promote the health and prevent death of RGCs post-injury[3,7,14,28,29]; however, investigation into the specific roles of HDACs 1, 2, and 3 in RGC chromatin remodeling is still lacking. MS-275, a selective HDAC1 inhibitor with modest activity against HDAC3, provided transient RGC protection in models of both ischemia[30] and optic nerve axotomy.[13] Knockdown of HDAC2 in a model of retinal ischemia prevented the loss of RGCs in the GCL and ameliorated electrophysiological responses.[6] Conditional knockout of *Hdacs* 1 and 2 in mouse RGCs also provided transient protection from axotomy.[31] In all these studies, however, only selective ablation[8] or selective inhibition of *Hdac3* (this study) has provided the greatest antiapoptotic effect in terms of numbers of surviving cells and length of effect. This implies that global chromatin changes associated with the apoptotic program is relatively more critical for continuation of the program. This creates something of a paradox for developing a protective strategy, suggesting that a trade-off between RGC function and survival is the likely goal of a treatment directed at HDAC activity. Alternatively, all available data to date have been collected from models of severe damage, creating the need to translate these findings to chronic models of optic nerve damage, such as experimental glaucoma.

The use of HDAC3 selective RGFP966 in an ONC model of axonal degeneration follows a precedent set by others in using HDAC isoform inhibitors to treat neurodegeneration in models of Huntington's, Friedreich's ataxia, cortical plasticity, and memory loss.[12,15,32–35] Importantly, specifically inhibiting HDAC3 activity has been shown to be protective in all of these neurodegenerative conditions. Further considerations of translating HDAC inhibitors, such as RGFP966, to a therapeutic use requires accurate dosing to both selectively target the neurotoxic activity of HDAC3 and to limit the chance of adverse side effects from the drug. This is especially important in chronic neurodegenerative conditions, where drug application may be required over the course of many years.

The most likely toxic effect of an HDAC inhibitor is expected to be on populations of cells in the body that are actively dividing. HDAC3 activity has been implicated in regulating both the S phase and late G2/M phase transition of the cell cycle.[36–38] Additionally, HDAC3 inhibitors are being developed as anticancer agents,[39,40] although these effects may not necessarily be mediated directly on the cell cycle.[41] Since any treatment for a chronic neurodegenerative condition such as glaucoma will likely be long lasting, it will be important to monitor other tissues for toxic side effects. In this study, we show that dosing mice systemically with 10 mg/kg RGFP966 daily for 2 weeks did not cause weight loss or histopathological effects such as inflammation or gross tissue damage. Additionally, we specifically monitored the effect on proliferation of rapidly dividing mucosal epithelial cells, which was not affected. These observations correlate with previous findings that RGFP966 was both nontoxic and protective at the effective dose of drug in other models of neurodegeneration.[12,34]

Vision loss in glaucoma is a result of chronic pathology at the optic nerve head often associated with increases in ocular hypertension.[42–45] The disease is characterized by asynchronous RGC loss over an extended period of time, often over the course of many years.[46] While glaucoma is a neurodegenerative condition, the only accepted treatments for this disease are focused on lowering intraocular pressure.[47] While this is clinically established to slow disease progression,[48,49] there is general acceptance that an effective therapy that targets the affected tissue would provide greater benefit to

patients when applied in conjunction with pressure-lowering treatments. Data collected in this study, have elucidated specific effective doses for intravitreal or IP administration of RGFP966 to protect against RGC death long after acute axonal injury, without causing toxicity. Further investigation is needed to interrogate the effect of prolonged RGFP966 treatment on RGC somatic survival and axonal degeneration in chronic models of glaucoma.

Acknowledgments

This work was supported by the National Eye Institute Grant R01 EY012223 (R.W.N.) and Vision Science CORE Grant P30 EY016665 (Department of Ophthalmology and Visual Sciences, University of Wisconsin), NRSA T32 grant GM081061, and unrestricted funding from Research to Prevent Blindness, Inc. (Department of Ophthalmology and Visual Sciences, University of Wisconsin). HDAC3-selective inhibitor, RGFP966, was provided as a gift by Repligen Corporation, Waltham, MA. The authors would also like to thank Mr. Nitin Kanneganti for assistance in conducting some of the experiments.

Author Disclosure Statement

No competing financial interests exist. RGFP966 was originally provided to R.W.N. from the Repligen Corporation. Rights to RGFP966 are now owned by BioMarin Pharmaceutical, Inc., who continues to provide reagent as a gift to the laboratory of the communicating author.

References

1. McKinnon, S.J., Schlamp, C.L., and Nickells, R.W. Mouse models of retinal ganglion cell death and glaucoma. *Exp. Eye Res*. 88:816–824, 2009.
2. Janssen, K.T., Mac Nair, C.E., Dietz, J.A., Schlamp, C.L., and Nickells, R.W. Nuclear atrophy of retinal ganglion cells precedes the bax-dependent stage of apoptosis. *Invest. Ophthalmol. Vis. Sci*. 54:1805–1815, 2013.
3. Pelzel, H.R., Schlamp, C.L., and Nickells, R.W. Histone H4 deacetylation plays a critical role in early gene silencing during neuronal apoptosis. *BMC Neurosci*. 11:62, 2010.
4. Wang, Z., Zang, C., Cui, K., et al. Genome-wide mapping of HATs and HDACs reveals distinct functions in active and inactive genes. *Cell*. 138:1019–1031, 2009.
5. Tiwari, S., Dharmarajan, S., Shivanna, M., Otteson, D.C., and Belecky-Adams, T.L. Histone deacetylase expression patterns in developing murine optic nerve. *BMC Dev. Biol*. 14:30, 2014.
6. Fan, J., Alsarraf, O., Dahrouj, M., et al. Inhibition of HDAC2 protects the retina from ischemic injury. *Invest. Ophthalmol. Vis. Sci*. 54:4072–4080, 2013.
7. Pelzel, H.R., Schlamp, C.L., Waclawski, M., Shaw, M.K., and Nickells, R.W. Silencing of *Fem1c*^{R3} gene expression in the DBA/2J mouse precedes retinal ganglion cell death and is associated with histone deacetylase activity. *Invest. Ophthalmol. Vis. Sci*. 53:1428–1435, 2012.
8. Schmitt, H.M., Pelzel, H.R., Schlamp, C.L., and Nickells, R.W. Histone deacetylase 3 (HDAC3) plays an important role in retinal ganglion cell death after acute optic nerve injury. *Mol. Neurodegener*. 9:39, 2014.
9. Bardai, F.H., and D'Mello, S.R. Selective toxicity by HDAC3 in neurons: regulation by Akt and GSK3beta. *J. Neurosci*. 31:1746–1751, 2011.
10. Bardai, F.H., Verma, P., Smith, C., et al. Disassociation of histone deacetylase-3 from normal huntingtin underlies mutant huntingtin neurotoxicity. *J. Neurosci*. 33:11833–11838, 2013.
11. Duncan, C.E., An, M.C., Papanikolaou, T., et al. Histone deacetylase-3 interacts with ataxin-7 and is altered in a spinocerebellar ataxia type 7 mouse model. *Mol. Neurodegener*. 8:42, 2013.
12. Malvaez, M., McQuown, S.C., Rogge, G.A., et al. HDAC3-selective inhibitor enhances extinction of cocaine-seeking behavior in a persistent manner. *Proc. Natl Acad. Sci. U. S. A*. 110:2647–2652, 2013.
13. Chindasub, P., Lindsey, J.D., Duong-Polk, K., Leung, C.K., and Weinreb, R.N. Inhibition of histone deacetylases 1 and 3 protects injured retinal ganglion cells. *Invest. Ophthalmol. Vis. Sci*. 54:96–102, 2013.
14. Alsarraf, O., Fan, J., Dahrouj, M., et al. Acetylation preserves retinal ganglion cell structure and function in a chronic model of ocular hypertension. *Invest. Ophthalmol. Vis. Sci*. 55:7486–7493, 2014.
15. Gottesfeld, J.M., Rusche, J.R., and Pandolfo, M. Increasing frataxin gene expression with histone deacetylase inhibitors as a therapeutic approach for Friedreich's ataxia. *J. Neurochem*. 126:147–154, 2013.
16. Li, Y., Schlamp, C.L., and Nickells, R.W. Experimental induction of retinal ganglion cell death in adult mice. *Invest. Ophthalmol. Vis. Sci*. 40:1004–1008, 1999.
17. Jiang, S.M., Zeng, L.P., Zeng, J.H., et al. Beta-III-Tubulin: a reliable marker for retinal ganglion cell labeling in experimental models of glaucoma. *Int. J. Ophthalmol*. 8:643–652, 2015.
18. Weishaupt, J.H., Klocker, N., and Bahr, M. Axotomy-induced early down-regulation of POU-IV class transcription factors Brn-3a and Brn-3b in retinal ganglion cells. *J. Mol. Neurosci*. 26:17–25, 2005.
19. Nadal-Nicolas, F.M., Jimenez-Lopez, M., Sobrado-Calvo, P., et al. Brn3a as a marker of retinal ganglion cells: qualitative and quantitative time course studies in naive and optic nerve-injured retinas. *Invest. Ophthalmol. Vis. Sci*. 50:3860–3868, 2009.
20. West, A.C., and Johnstone, R.W. New and emerging HDAC inhibitors for cancer treatment. *J. Clin. Invest*. 124:30–39, 2014.
21. Radhakrishnan, K., Sonali, N., Moreno, M., et al. Protein delivery to the back of the eye: barriers, carriers and stability of anti-VEGF proteins. *Drug Discov Today*. 2016.
22. Thoongsuwan, S., Dawn Lam, H.H., and Bhisitkul, R.B. Bleb-associated infections after intravitreal injection. *Retin. Cases Brief Rep*. 5:315–317, 2011.
23. Maurice, D.M., Mishima, S. Ocular pharmacokinetics. *Handb. Exp. Pharmacol*. 69:19–116, 1984.
24. Shultz, M.D., Cao, X., Chen, C.H., et al. Optimization of the in vitro cardiac safety of hydroxamate-based histone deacetylase inhibitors. *J. Med. Chem*. 54:4752–4772, 2011.
25. Dietz, K.C., and Casaccia, P. HDAC inhibitors and neurodegeneration: at the edge between protection and damage. *Pharmacol. Res*. 62:11–17, 2010.
26. Schlamp, C.L., Johnson, E.C., Li, Y., Morrison, J.C., and Nickells, R.W. Changes in Thy1 gene expression associated with damaged retinal ganglion cells. *Mol. Vis*. 7:192–201, 2001.
27. Semaan, S.J., Li, Y., and Nickells, R.W. A single nucleotide polymorphism in the Bax gene promoter affects transcription and influences retinal ganglion cell death. *ASN Neuro*. 2:e00032, 2010.

28. Biermann, J., Boyle, J., Pielen, A., and Lagreze, W.A. Histone deacetylase inhibitors sodium butyrate and valproic acid delay spontaneous cell death in purified rat retinal ganglion cells. *Mol. Vis*. 17:395–403, 2011.
29. Zhang, Z.Z., Gong, Y.Y., Shi, Y.H., et al. Valproate promotes survival of retinal ganglion cells in a rat model of optic nerve crush. *Neuroscience*. 224:282–293, 2012.
30. Murphy, S.P., Lee, R.J., McClean, M.E., et al. MS-275, a class I histone deacetylase inhibitor, protects the p53-deficient mouse against ischemic injury. *J Neurochem*. 129: 509–515, 2014.
31. Lebrun-Julien, F., and Suter, U. Combined HDAC1 and HDAC2 depletion promotes retinal ganglion cell survival after injury through reduction of p53 target gene expression. *ASN Neuro*. 7:pii:1759091415593066, 2015.
32. Dompierre, J.P., Godin, J.D., Charrin, B.C., et al. Histone deacetylase 6 inhibition compensates for the transport deficit in Huntington's disease by increasing tubulin acetylation. *J. Neurosci*. 27:3571–3583, 2007.
33. Jia, H., Pallos, J., Jacques, V., et al. Histone deacetylase (HDAC) inhibitors targeting HDAC3 and HDAC1 ameliorate polyglutamine-elicited phenotypes in model systems of Huntington's disease. *Neurobiol. Dis*. 46:351–361, 2012.
34. Jia, H., Wang, Y., Morris, C.D., et al. The effects of pharmacological inhibition of histone deacetylase 3 (HDAC3) in Huntington's disease mice. *PLoS One*. 11: e0152498, 2016.
35. Shan, B., Xu, C., Zhang, Y., et al. Quantitative proteomic analysis identifies targets and pathways of a 2-aminobenzamide HDAC inhibitor in Friedreich's ataxia patient iPSC-derived neural stem cells. *J. Proteome Res*. 13:4558–4566, 2014.
36. Jiang, Y., and Hsieh, J. HDAC3 controls gap 2/mitosis progression in adult neural stem/progenitor cells by regulating CDK1 levels. *Proc. Natl Acad. Sci. U. S. A*. 111: 13541–13546, 2014.
37. Patil, H., Wilks, C., Gonzalez, R.W., et al. Mitotic activation of a novel histone deacetylase 3-linker histone H1.3 protein complex by protein kinase CK2. *J. Biol. Chem*. 291: 3158–3172, 2016.
38. Vidal-Laliena, M., Gallastegui, E., Mateo, F., et al. Histone deacetylase 3 regulates cyclin A stability. *J. Biol. Chem*. 288:21096–21104, 2013.
39. Godman, C.A., Joshi, R., Tierney, B.R., et al. HDAC3 impacts multiple oncogenic pathways in colon cancer cells with effects on Wnt and vitamin D signaling. *Cancer Biol. Ther*. 7:1570–1580, 2008.
40. Khabele, D., Son, D.S., Parl, A.K., et al. Drug-induced inactivation or gene silencing of class I histone deacetylases suppresses ovarian cancer cell growth: implications for therapy. *Cancer Biol. Ther*. 6:795–801, 2007.
41. Wilson, A.J., Byun, D.S., Popova, N., et al. Histone deacetylase 3 (HDAC3) and other class I HDACs regulate colon cell maturation and p21 expression and are deregulated in human colon cancer. *J. Biol. Chem*. 281:13548–13558, 2006.
42. Fortune, B., Burgoyne, C.F., Cull, G.A., Reynaud, J., and Wang, L. Structural and functional abnormalities of retinal ganglion cells measured in vivo at the onset of optic nerve head surface change in experimental glaucoma. *Invest. Ophthalmol. Vis. Sci*. 53:3939–3950, 2012.
43. Gardiner, S.K., Fortune, B., Wang, L., Downs, J.C., and Burgoyne, C.F. Intraocular pressure magnitude and variability as predictors of rates of structural change in nonhuman primate experimental glaucoma. *Exp. Eye Res*. 103: 1–8, 2012.
44. Nickells, R.W. Retinal ganglion cell death in glaucoma: the how, the why, and the maybe. *J. Glaucoma*. 5:345–356, 1996.
45. Quigley, H.A., Nickells, R.W., Kerrigan, L.A., et al. Retinal ganglion cell death in experimental glaucoma and after axotomy occurs by apoptosis. *Invest. Ophthalmol. Vis. Sci*. 36:774–786, 1995.
46. De Moraes, C.G., Liebmann, J.M., and Levin, L.A. Detection and measurement of clinically meaningful visual field progression in clinical trials for glaucoma. *Prog. Retin. Eye Res*. 2016.
47. Quigley, H.A. Glaucoma. *Lancet*. 377:1367–1377, 2011.
48. Pandey, A.N., and Sujata, S. Study of long term structural and functional changes in medically controlled glaucoma. *Int. J. Ophthalmol*. 7:128–132, 2014.
49. Parrish, R.K., 2nd, Feuer, W.J., Schiffman, J.C., et al. Five-year follow-up optic disc findings of the Collaborative Initial Glaucoma Treatment Study. *Am. J. Ophthalmol*. 147: 717–724.e1, 2009.

Received: May 19, 2017
Accepted: October 16, 2017

Address correspondence to:
Dr. Robert W. Nickells
Department of Ophthalmology and Visual Sciences
University of Wisconsin-Madison
571A MSC, 1300 University Avenue
Madison, WI 53706

E-mail: nickells@wisc.edu